

## MECHANISM AND KINETICS OF THE REACTION 1 DOLOMITE + 2 QUARTZ = 1 DIOPSIDE + 2 CO<sub>2</sub> INVESTIGATED BY POWDER EXPERIMENTS

ANDREAS LÜTTGE AND PAUL METZ

*Institut für Mineralogie, Petrologie und Geochemie, Universität Tübingen, Wilhelmstr. 56,  
D-7400 Tübingen, Germany*

### ABSTRACT

Experimental investigation of the forward reaction 1 dolomite + 2 quartz = 1 diopside + 2 CO<sub>2</sub> was carried out in a conventional hydrothermal apparatus, in order to determine the mechanism and the kinetics at a total pressure of 500 MPa and 680°C. The CO<sub>2</sub> contents of the fluid phase, consisting of carbon dioxide and water, was found to vary from 80 to nearly 100 mol%. The experiments lasted up to 365 days (8,760 hours). SEM examination of the reaction mixtures clearly shows a dissolution - crystallization mechanism operating within the whole range of  $X(\text{CO}_2)$ , even at almost "dry" conditions. The data on degree of conversion *versus* time, results of SEM studies of experiments, and a variation of surface area of reactants and products, have shown that rate-limiting processes are always interface-controlled as long as the diopside crystals do not cover the dolomite surfaces completely. During the first 600-800 hours, the rate of the heterogeneous reaction is controlled by the interplay of dolomite dissolution and diopside crystallization (including nucleation and growth). Compared with these processes, quartz dissolution appears to be rapid in any case under the experimental conditions applied. All of these dissolution and crystallization "steps" are themselves complex processes that consist of several elementary reactions. The experimental results show that the rate-limiting process changes during the course of reaction, even if P-T- $X(\text{CO}_2)$  conditions are constant, or nearly constant. At the beginning of the reaction, diopside crystallization is rate-limiting, but later, dolomite dissolution becomes rate-determining; finally, when the dolomite-armoring diopside rim is complete (~800 hours, ~35% conversion), the transport of dissolved species through the armoring rim becomes the rate-limiting step. In addition, the essential catalytic effect of water was verified in our experiments.

**Keywords:** kinetics, quartz, dolomite, diopside, SEM, rate control, surface control, reaction mechanism.

### SOMMAIRE

Nous avons étudié la réaction 1 dolomite + 2 quartz = 1 diopside + 2 CO<sub>2</sub> au moyen d'expériences avec appareillage hydrothermal conventionnel, afin de déterminer le mécanisme et la cinétique de cette réaction à 500 MPa et 680°C. La teneur en CO<sub>2</sub> de la phase fluide,

mélange de CO<sub>2</sub> et de H<sub>2</sub>O, varie entre 80 et presque 100%. Les expériences ont duré jusqu'à 365 jours (8,760 heures). Un examen des mélanges au microscope électronique à balayage (MEB) démontre clairement un mécanisme de dissolution et de cristallisation pour toute valeur de  $X(\text{CO}_2)$ , même dans les situations presque anhydres. Les données sur le degré de conversion en fonction du temps et l'évidence au MEB, pour une surface spécifique variable des réactifs et des produits, montrent que les processus qui limitent le taux de réaction sont toujours régis par l'interface, pourvu que les cristaux de diopside ne recouvrent pas entièrement les grains de dolomite. Pendant les 600 à 800 premières heures, le taux de réaction hétérogène dépend de l'interaction de la dissolution de la dolomite et la cristallisation (y inclus nucléation et croissance) de la diopside. Comparée à ces processus, la dissolution du quartz semble très rapide dans toutes les conditions expérimentales étudiées. Toutes ces "étapes" de dissolution et de cristallisation sont elles-mêmes des processus complexes qui comprennent plusieurs réactions élémentaires. Les résultats expérimentaux montrent que l'identité du processus le plus lent change au cours de l'expérience, même où les conditions P-T- $X$  sont constantes, ou à peu près. Au début de la réaction, le taux de cristallisation de la diopside limite le progrès de la réaction; plus tard, ce sera la dissolution de la dolomite qui en limite le progrès. Une fois l'armure de dolomite autour de la diopside complétée (~800 heures, ~35% de conversion), le transfert des espèces dissoutes à travers le liseré devient le processus qui limite le progrès de la réaction. De plus, nous avons confirmé l'influence catalytique essentielle de l'eau.

(Traduit par la Rédaction)

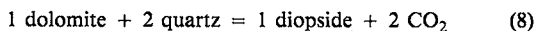
**Mots-clés:** cinétique, quartz, dolomite, diopside, microscopie électronique à balayage, contrôle du taux de réaction, contrôle de la surface, mécanisme de réaction.

### INTRODUCTION

During the last three decades, the P-T- $X$  conditions of stability of numerous mineral assemblages have been determined. The resulting petrogenetic grids allow us to quantify the equilibrium conditions of many metamorphic reactions. Then "the focus of metamorphic petrology

shifted... ..to a dynamic mode aimed at the quantification of the processes that produced the metamorphism" (Lasaga 1986), *i.e.*, to questions related to mechanisms and time dependence. One of the pioneering experimental studies of the mechanism and kinetics of a metamorphic mineral reaction was carried out by Greenwood (1963). Since then, several heterogeneous mineral reactions have been investigated, *e.g.*, by Kridelbaugh (1973), Matthews (1980, 1985), Tanner *et al.* (1985), Rubie (1986), Rubie & Brearley (1987), Lüttge *et al.* (1987), Schramke *et al.* (1987), Dachs & Metz (1988) and Heinrich *et al.* (1989).

As pointed out in many of the papers mentioned above, the dissolution of reactant minerals, along with the transport of dissolved species, are important processes in the kinetics of heterogeneous reactions among minerals. Consequently, much work has been devoted to understanding mineral dissolution, *e.g.*, by Berner (1978), Berner & Holdren (1979), Berner & Morse (1974), Berner & Schott (1982), Berner *et al.* (1980), Eugster (1982, 1986), Fein & Walther (1987), Novgorodov (1975), Petrovich (1976, 1981a,b), Rimstidt & Barnes (1980), Walther & Orville (1982, 1983) and Blum *et al.* (1990). Our investigations of the mechanism and kinetics of a "simple" decarbonation reaction, number (8) in the system CaO - MgO - SiO<sub>2</sub> - CO<sub>2</sub> - H<sub>2</sub>O (Winkler 1979, p. 116),



contributes to the body of work directed toward an understanding of the kinetics of metamorphic reactions.

#### EXPERIMENTAL METHODS

Figure 1A shows the optically clear natural

dolomite (Algeria) with a Fe content of 0.7 wt% FeO (Heinrich *et al.* 1986) and a single crystal of synthetic quartz (Kristallverarbeitende Gesellschaft, Neckar-Bischofsheim: Toyocom 1975), which were used to prepare the starting mixtures (40 mg). The stoichiometry of the reaction requires 60.5 wt% (24.22 mg) CaMg(CO<sub>3</sub>)<sub>2</sub> and 39.5 wt% (15.78 mg) SiO<sub>2</sub>. All cleavage pieces of dolomite (Dol) and irregularly shaped quartz grains (Qtz) had a specific grain-size distribution (given below, and see Fig. 1B) produced by ultrasonic sieving. A special, improved method of achieving run conditions (*e.g.*, Tanner *et al.* 1985) was not necessary, because the grinding of powders could not be observed to exert any influence by SEM methods. The powders used for the unseeded runs H08-H50 and experiments H73-H82, which contained diopside seeds, had an 80-100 μm grain-size distribution between 80 and 100 μm. In runs H57-H66, 20 mg of the dolomite had a grain size of 5-10 μm, and the remaining 4.22 mg dolomite, and all the quartz, had a grain size of 80-100 μm. In contrast, runs H67-H72 were carried out with 13 mg of quartz from the 5-10 μm size fraction plus 2.78 mg quartz and all dolomite from the 80-100 μm size fraction.

The fluid phase (10 mg) used in the runs mentioned above consisted of water and carbon dioxide [ $X(\text{CO}_2) = 0.90$ ]; it was produced by decomposition of silver oxalate (Ag<sub>2</sub>C<sub>2</sub>O<sub>4</sub>). Low H<sub>2</sub>O contents of the very fine-grained Ag<sub>2</sub>C<sub>2</sub>O<sub>4</sub> have to be considered even after several days of drying at 60°C in the vacuum.

All experiments were carried out in a conventional hydrothermal apparatus (cold-seal pressure vessel). The experiments with CO<sub>2</sub> and H<sub>2</sub>O were run in sealed gold capsules. P-T conditions for these experiments were 500 MPa ± 5 MPa and 680°C ± 3°C (see also Heinrich *et al.* 1986). The equilibrium temperature of the reaction at 500 MPa

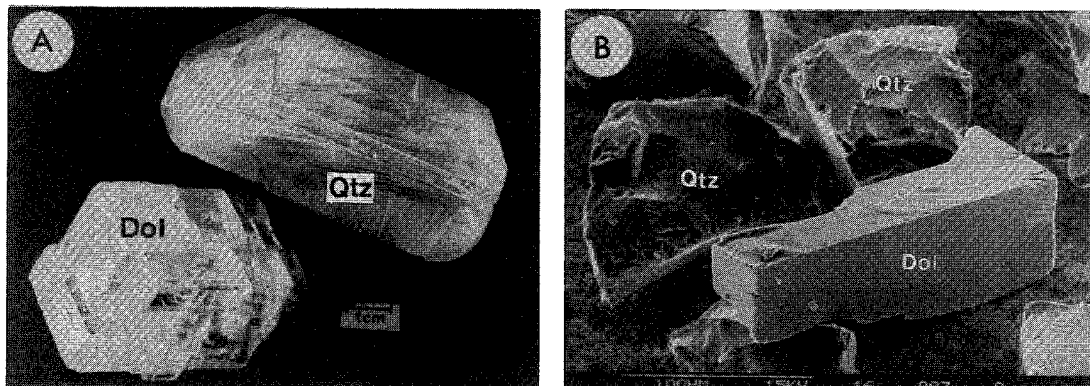


FIG. 1. Starting materials. A. Photo of the synthetic quartz (Qtz) and natural dolomite (Dol) from Algeria, used to prepare all starting mixtures. B. SEM photo showing a part of the starting mixture: a cleavage piece of dolomite and two grains of quartz, all from the 80-100 μm grain-size fraction.

and  $X(\text{CO}_2) = 0.9$  is  $615^\circ\text{C} \pm 5^\circ\text{C}$  (Gottschalk 1990; see also Fig. 2, curve 8). Thus, the equilibrium temperature was overstepped by approximately  $65^\circ\text{C}$ . The temperature was measured

with a calibrated chromel–alumel thermocouple situated inside the autoclaves and in direct contact with the central part of the gold capsules. Run durations were varied from 10 to nearly 3,000

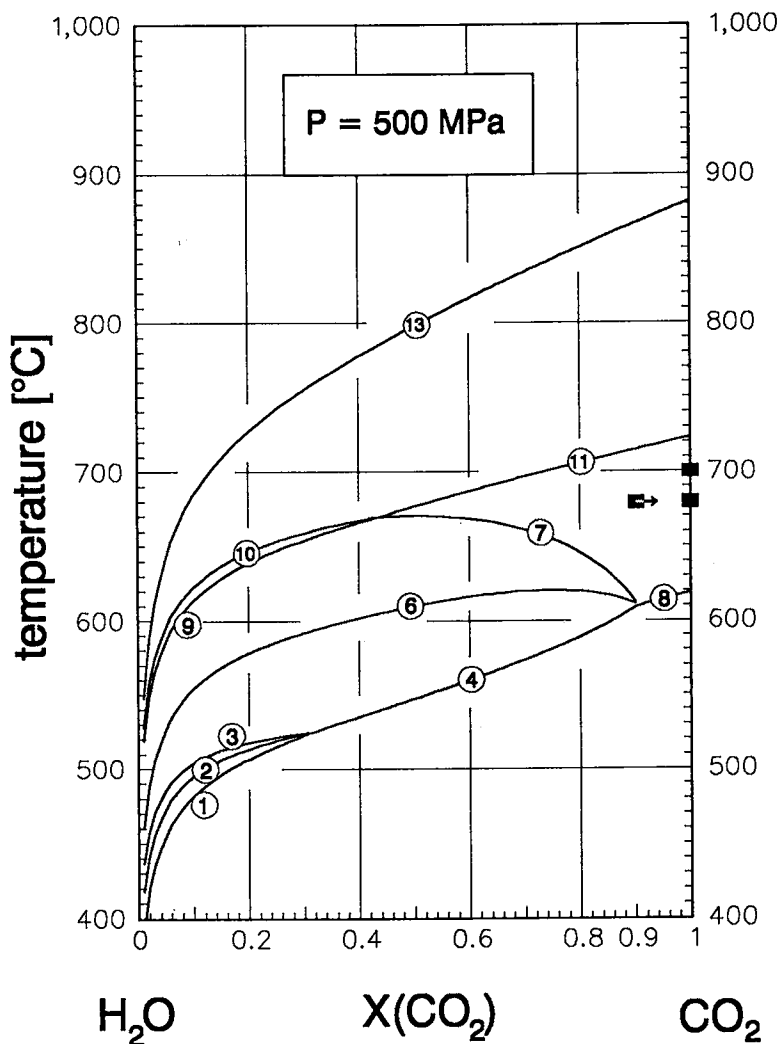


FIG. 2. Isobaric T-X diagram ( $P = 500 \text{ MPa}$ ) for the system  $\text{CaO-MgO-SiO}_2\text{-CO}_2\text{-H}_2\text{O}$ , with calculated equilibria for reactions (1)–(13) (Gottschalk 1990). Curve (8) shows the equilibrium conditions for the reaction investigated, and the black square indicates experimental T-X( $\text{CO}_2$ ) conditions. The arrow shows the direction and highest magnitude of  $X(\text{CO}_2)$  shift during all runs performed. 3 Dol + 4 Qtz + 1  $\text{H}_2\text{O}$  = 1 Tlc + 3 Cal + 3  $\text{CO}_2$  (1), 5 Tlc + 6 Cal + 4 Qtz = 3 Tr + 6  $\text{CO}_2$  + 2  $\text{H}_2\text{O}$  (2), 2 Tlc + 3 Cal = 1 Tr + 1 Dol + 1  $\text{CO}_2$  + 1  $\text{H}_2\text{O}$  (3), 5 Dol + 8 Qtz + 1  $\text{H}_2\text{O}$  = 1 Tr + 3 Cal + 7  $\text{CO}_2$  (4), 1 Tr + 3 Cal + 2 Qtz = 5 Di + 3  $\text{CO}_2$  + 1  $\text{H}_2\text{O}$  (6), 1 Tr + 3 Cal = 4 Di + 1 Dol + 1  $\text{CO}_2$  + 1  $\text{H}_2\text{O}$  (7), 1 Do + 2 Qtz = 1 Di + 2  $\text{CO}_2$  (8), 1 Tr + 11 Dol = 8 Fo + 13 Cal + 9  $\text{CO}_2$  + 1  $\text{H}_2\text{O}$  (9), 3 Tr + 5 Cal = 11 Di + 2 Fo + 5  $\text{CO}_2$  + 3  $\text{H}_2\text{O}$  (10), 1 Di + 3 Dol = 2 Fo + 4 Cal + 2  $\text{CO}_2$  (11), 2 Cal + 2 Qtz = 1 Wo + 2  $\text{CO}_2$  (13). Symbols: Cal calcite, Di diopside, Dol dolomite, Fo forsterite, Qtz quartz, Tlc talc, Tr tremolite, Wo wollastonite.

hours, *i.e.*, up to 125 days. Reaction progress [= conversion  $\alpha$  (0–100%)] was determined by weighing the amount of  $\text{CO}_2$  formed (*e.g.*, Käse & Metz 1980) and using the stoichiometry of reaction (8). The  $\text{CO}_2$  was weighed with a Sartorius MP8 Ultra Micro Balance with an accuracy of better than 1%. The  $\text{CO}_2$  content of the fluid phase increased 4 mol% during the runs [ $X(\text{CO}_2) = 0.94$ ]. This procedure of determining the extent of conversion is correct, so long as reaction (8) is the only reaction. All solid phases were examined by optical, SEM (Stereoscan 250), EDX and X-ray powder diffraction. In specific cases, TEM and electron-microprobe analysis (ARL) also were used. No solid phases other than quartz, dolomite and diopside have been detected by X-ray diffraction. By utilizing SEM studies, metastable formation of talc was observed. The talc content is in any case so small that the error in the conversion measurement referred to above is not more than 0.5% absolute.

For comparison, experiments also were carried out with a fluid phase of nearly pure  $\text{CO}_2$ , without addition of water. In this case, the pressure medium, which was carbon dioxide (99.995%  $\text{CO}_2$ ), also served as the fluid phase, because earlier results had shown that  $\text{Ag}_2\text{C}_2\text{O}_4$  always contains water, which cannot be expelled and which moves the  $X(\text{CO}_2)$  to values somewhat lower than 1. This is in agreement with results obtained by Tanner *et al.* (1985). Therefore,  $\text{CO}_2$  from the pressure medium was introduced into the gold capsules *via* a small tube-like channel. The disadvantage of

infiltration of nickel and chromium into the capsules is negligible during a run duration up to 182 days and is offset by the advantage of "dry"  $\text{CO}_2$ .

## EXPERIMENTAL RESULTS

### Mixed $\text{CO}_2$ - $\text{H}_2\text{O}$ fluids

Results of experiments involving mixed  $\text{CO}_2$ - $\text{H}_2\text{O}$  fluids are given in Tables 2, 3, and 4, along with the experimental conditions; Table 1 lists the definition of symbols used here. SEM photos of run products are given in Figures 3A–D, 4A–F, and 10A. Figures 5–8 show the results of the experiments designed to investigate extent of conversion with time, and Figure 9 gives the results of

TABLE 2. EXPERIMENTAL DATA OF THE CONVERSION-TIME EXPERIMENTS CARRIED OUT AT 500 MPa

run No.	T [°C]	t [h]/[d]	mg solid	X(CO <sub>2</sub> ) start	X(CO <sub>2</sub> ) final	CO <sub>2</sub> -prod. [mg]	conver. [%]
H08	680	20/1	38.79	0.90	0.90	0.13	1
H09	680	20/1	39.00	0.90	0.90	0.05	0.5
H10	680	45/2	39.73	0.90	0.91	0.93	8
H11*	680	45/2	40.30	0.90	—	—	—
H12	680	50/2	39.69	0.90	0.91	0.74	6
H13	680	50/2	39.34	0.90	0.91	1.03	9
H14	680	71/3	39.72	0.90	0.91	0.82	7
H15	680	71/3	39.06	0.90	0.90	0.53	5
H16	680	90/4	39.37	0.90	0.91	0.59	5
H17	680	90/4	39.53	0.90	0.91	1.03	9
H18**)	680	95/4	39.39	0.90	0.91	0.79	7
H19	680	95/4	38.84	0.90	0.91	1.47	13
H20**	680	96/4	39.41	0.90	—	—	—
H21	680	120/5	39.69	0.90	0.91	1.32	12
H22	680	120/5	40.48	0.90	0.92	3.13	27
H23	680	192/8	40.21	0.90	0.91	1.69	15
H24	680	192/8	39.86	0.90	0.91	1.46	13
H25	680	200/8	37.97	0.90	0.91	1.42	13
H26	680	200/8	39.04	0.90	0.91	1.77	16
H27	680	239/10	39.90	0.90	0.91	1.20	10
H28	680	239/10	37.64	0.90	0.91	1.76	15
H29	680	240/10	39.39	0.90	0.92	2.76	26
H30	680	240/10	39.28	0.90	0.92	2.34	21
H31	680	288/12	40.10	0.90	0.92	2.31	20
H32	680	288/12	39.73	0.90	0.92	2.89	25
H33	680	346/14	39.81	0.90	0.92	3.18	28
H34	680	346/14	39.37	0.90	0.92	3.38	30
H35	680	358/15	39.30	0.90	0.92	3.13	28
H36	680	358/15	39.32	0.90	0.92	2.81	25
H37	680	400/17	39.07	0.90	0.92	3.27	29
H38	680	400/17	39.62	0.90	0.92	2.96	26
H39	680	450/19	39.25	0.90	0.92	3.27	29
H40	680	450/19	39.67	0.90	0.92	3.37	29
H41	680	515/21	39.85	0.92	0.94	3.11	27
H42	680	515/21	40.14	0.90	0.92	3.64	31
H43	680	600/25	39.89	0.90	0.92	3.46	30
H44	680	600/25	39.75	0.90	0.92	3.50	30
H45*	680	1000/42	38.49	0.90	—	—	—
H46*	680	1000/42	39.84	0.90	—	—	—
H47	680	1950/81	39.05	0.90	0.93	5.18	46
H48	680	1950/81	39.26	0.90	0.93	4.77	42
H49*	680	2950/123	38.92	0.90	—	—	—
H50	680	2950/123	39.06	0.90	0.93	5.48	49

All experiments started off with 10 mg of a  $\text{CO}_2$ - $\text{H}_2\text{O}$  fluid phase [ $X(\text{CO}_2) = 0.90$ ] and with 40 mg of a mixture of 60.5% by weight of dolomite and 39.5% of quartz. The starting mixture of dolomite and quartz had always an 80–100  $\mu\text{m}$  grain fraction. \* Gold capsule was leaky at the end of the run; SEM study only. \*) 1 mg calcite (grain-size fraction: 20–40  $\mu\text{m}$ ) was added. \*\* "blow-quench" experiment (pressure is lowered very rapidly to 0.1 MPa before quenching the temperature, with the result that the capsule breaks, and the fluid phase escapes from the capsule).

TABLE 1. DEFINITION OF SYMBOLS USED

A	= surface area of mineral
$a_i$	= activity of species <i>i</i>
$a(\text{H}^+)$	= activity of $\text{H}^+$
$c_i$	= concentration of species <i>i</i>
<i>i</i>	= species <i>i</i> in solution or in mineral, respectively
$K_{\text{eq}}$	= reaction equilibrium constant
$k^+$	= rate constant of dissolution of mineral
$L^*$	= concentration product
$L_{\Theta}^{\text{eq}}$	= reduced concentration product of mineral $\Theta$ at equilibrium
$L_{\text{Di nucleation}}$	= value has to be overstepped to induce nucleation of diopside
<i>m</i>	= constant (experimentally determined)
<i>m</i>	= constant (experimentally determined)
P	= pressure (MPa)
Q	= activity quotient
T	= temperature (°C)
t	= time (hours)
V	= volume of the solution (fluid phase) in contact with mineral
$X(i)$	= mole fraction of species <i>i</i>
$\alpha$	= conversion (%)
$\nu_{\Theta}$	= stoichiometric coefficient of species "i" in mineral $\Theta$
$\Theta$	= mineral

TABLE 3. EXPERIMENTAL DATA PERTAINING TO DEGREE OF CONVERSION AS A FUNCTION OF TIME AT 500 MPa, WITH A VARIATION IN GRAIN SIZE

run No.	T [°C]	t [h]/[d]	mg solid	X(CO <sub>2</sub> ) start	X(CO <sub>2</sub> ) final	CO <sub>2</sub> -prod. [mg]	conver. [%]
H57	680	50/2	39.08	0.90	0.91	0.99	9
H58	680	50/2	39.35	0.90	0.91	0.68	6
H59	680	88/4	39.36	0.90	0.91	0.77	7
H60	680	88/4	39.58	0.90	0.91	1.50	13
H61	680	120/5	39.20	0.90	0.92	3.05	27
H62	680	120/5	39.65	0.90	0.92	2.51	22
H63	680	400/17	39.02	0.90	0.93	4.33	38
H64	680	400/17	39.22	0.90	0.93	4.61	41
H65	680	800/33	38.83	0.90	0.93	5.22	47
H66	680	800/33	32.98	0.90	0.93	4.62	42

TABLE 3b.

run No.	T [°C]	t [h]/[d]	mg solid	X(CO <sub>2</sub> ) start	X(CO <sub>2</sub> ) final	CO <sub>2</sub> -prod. [mg]	conver. [%]
H73	680	95/4	41.75	0.90	0.92	2.36	21
H74	680	95/4	42.56	0.90	0.91	1.64	14
H77	680	120/5	38.69	0.90	0.92	2.09	19
H78	680	120/5	39.70	0.90	0.91	1.85	16
H79	680	120/5	38.99	0.90	0.92	2.13	19
H80	680	120/5	38.84	0.90	0.91	1.94	17
H81	680	240/10	39.92	0.90	0.92	3.26	28
H82	680	430/18	38.96	0.90	0.93	4.41	39
H83	680	430/18	39.55	0.90	0.93	4.06	37

TABLE 3c.

run No.	T [°C]	t [h]/[d]	mg solid	X(CO <sub>2</sub> ) start	X(CO <sub>2</sub> ) final	CO <sub>2</sub> -prod. [mg]	conver. [%]
H67	680	120/5	39.68	0.90	0.91	1.37	12
H68	680	120/5	39.19	0.90	0.91	0.96	9
H69	680	200/8	39.13	0.90	0.91	1.70	15
H70	680	200/8	38.32	0.90	0.91	1.38	13
H71	680	436/18	39.11	0.90	0.92	2.21	20
H72	680	436/18	37.95	0.90	0.92	2.46	22

3a. All the quartz and 4.22 mg of the dolomite had an 80-100 μm grain size fraction, but the last 20 mg of dolomite grains were 5-10 microns in size.

3b. Diopside-seeded runs; 5 mg of diopside in a grain size fraction smaller 10 microns have been added.

3c. All the dolomite and 2.78 mg of quartz had an 80-100 μm grain size fraction, but the last 13 mg of quartz grains were 5-10 microns in size.

TABLE 4. EXPERIMENTAL DATA OF THE CONVERSION-TIME EXPERIMENTS CARRIED OUT AT 500 MPa WITH A VARIATION OF X(CO<sub>2</sub>)-START

run No.	T [°C]	t [h]/[d]	mg solid	X(CO <sub>2</sub> ) start	X(CO <sub>2</sub> ) final	CO <sub>2</sub> -prod. [mg]	conver. [%]
V/2	680	504/21	40.00	0.80	0.87	6.13	54
V/3	680	504/21	39.67	0.80	0.87	5.98	52
H42	680	515/21.5	40.14	0.90	0.92	3.64	31
H41	680	515/21.5	39.85	0.92	0.94	3.11	27
VII/3	680	504/21	38.93	0.95	0.95	2.58	23
VII/4	680	504/21	40.16	0.95	0.95	1.83	16

The starting mixture of dolomite and quartz had always an 80-100 μm grain size fraction. The value of X(CO<sub>2</sub>)-start was varied.

experiments carried out with different starting values of X(CO<sub>2</sub>).

### Pure CO<sub>2</sub> fluids

All experimental parameters of runs carried out using pure carbon dioxide (99.995% CO<sub>2</sub>) as fluid phase are given in Table 5. The exact value of conversion is not determinable, because gravimetric methods cannot be used on account of the open capsules. Thus, it was only possible to estimate the extent of conversion from SEM studies of reaction mixtures. The results are also given in Figure 9.

TABLE 5. EXPERIMENTAL DATA OF THE EXPERIMENTS CARRIED OUT WITH A FLUID PHASE OF PURE CO<sub>2</sub>

run No.	P [MPa]	T [°C]	t [h]/[d]	mg solid	X(CO <sub>2</sub> ) start	X(CO <sub>2</sub> ) final	CO <sub>2</sub> -prod. [mg]	conver. [%]
VI/3	500	680	1008/42	39.20	1.0	1.0	?	"1"
VI/9	300	700	1008/42	39.55	1.0	1.0	?	"2"
VI/7	300	750	1008/42	37.76	1.0	1.0	?	"5"
H84	500	700	4368/182	39.55	1.0	1.0	?	"3"
H85	500	680	8760/365	39.55	1.0	1.0	?	"3"

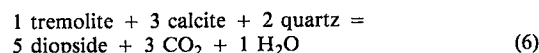
The starting mixture of dolomite and quartz had always an 80-100 μm grain fraction. The value of X(CO<sub>2</sub>) was nearly 1. Extent of conversion is only assessable and not determinable, because gravimetric methods cannot be used on account of the open capsules (see text).

The SEM photos (Figs. 10B-F) show some characteristic aspects of the reaction mechanism operating under "dry" conditions.

## DISCUSSION OF EXPERIMENTAL RESULTS

### Mixed CO<sub>2</sub>-H<sub>2</sub>O fluids

Some representative observations concerning the reaction mechanism are shown in Figures 3A to D: the diopside (Di) crystals nucleate and grow exclusively (with one exception, see below) on the dolomite surfaces (Fig. 3A), beginning at the edges, corners and probably at sites of dislocations. At 680°C, but even at 650°C, no nucleation barrier was observed for diopside, as was the case in the work of Dachs & Metz (1988) on the diopside-forming reaction, numbered (6) in the system CaO - MgO - SiO<sub>2</sub> - CO<sub>2</sub> - H<sub>2</sub>O (see Fig. 2):



The newly formed diopside crystals usually range from stalk-like to needle-like (Fig. 3B), and "whiskers" also can be observed. [By "whiskers", we do not mean crystals grown by special growth-mechanism (e.g. spiral growth), which cannot be investigated with the methods used, but rather the long hair-like diopside crystals that can be found in all reaction mixtures. We are not, therefore, using the term "whisker" in the narrow sense.] The surfaces of the dolomite not covered with diopside show dissolution features such as etch pits and terraced steps (Fig. 3D). The quartz grains (Figs. 3A, B), however, are nearly free of diopside crystals. Their surfaces are generally characterized by the development of facets. In addition, etch pits with a 2-fold symmetry (Lüttge & Metz, in prep.) and dissolution spikes (see Fig. 3B and Tanner *et al.* 1985, plate 2b), called "hillocks" (Heimann 1975), are very common. The exception referred to above consists of nucleation of diopside crystals on the top of some hillocks, which are the sites on the mineral surface having the slowest rate of removal

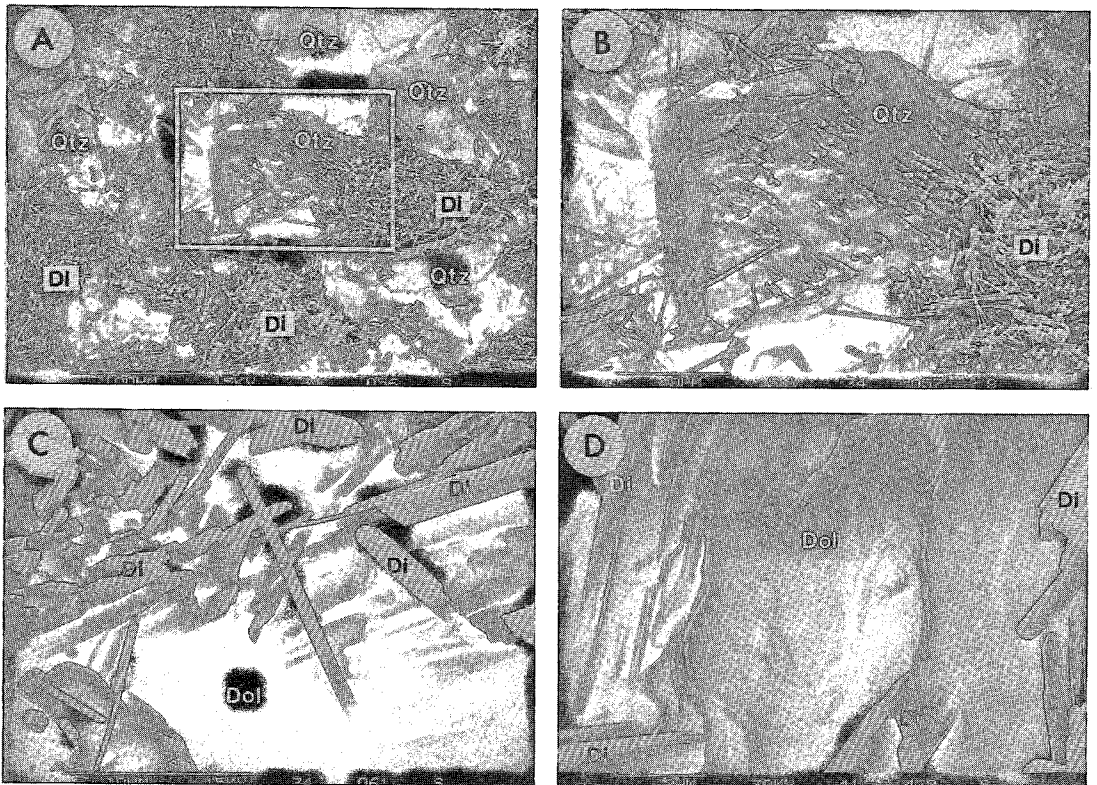


FIG. 3. A. Reaction mixture after 358 h at run conditions (H36,  $\alpha = 25\%$ ); surfaces of dolomite are covered by diopside (Di), whereas the quartz grains are completely uncovered. B. Quartz grain from A at a higher magnification, showing a special type of dissolution feature: hillocks. C. Stem-like to needle-like crystals of Di have grown on the dolomite surfaces, which become dissolved. D. Dissolution features (etch pits, terraced steps) on a surface of dolomite (H62,  $\alpha = 22\%$ ).

during dissolution.

From these textures, we conclude that the overall reaction mechanism occurs by dissolution – crystallization, as has also been suggested, *e.g.*, by Matthews (1980, 1985), Tanner *et al.* (1985), Heinrich *et al.* (1986), Lüttge *et al.* (1987), and Schramke *et al.* (1987) for some other reactions involving metamorphic minerals investigated by powder methods. It should be emphasized that many observations concerning the mechanism of the reaction investigated here are either comparable, or nearly identical, to those made by Tanner *et al.* (1985) during their study of the kinetics of the reaction: 1 calcite + 1 quartz = 1 wollastonite + 1 CO<sub>2</sub>.

Figure 11 shows schematically a simple two-path reaction model, as was also used by Dachs & Metz (1988) in a similar fashion. The overall mechanism of reaction consists of the dissolution of dolomite and quartz, transport of dissolved species through the fluid phase, and nucleation and growth of the diopside crystals. It is clear that each of these main processes may, in turn, consist of a reaction or a

sequence of reactions, as shown, for example, by Rimstidt & Barnes (1980) in the case of quartz dissolution. This means that the overall heterogeneous reaction is composed of one or more complex reactions or processes (dissolution, precipitation), which consist, in turn, of a number of elementary reactions.

#### KINETICS: EXPERIMENTAL

It is evident from a study of the literature that there is little agreement concerning the identity of the process(es) that control(s) the kinetics of a heterogeneous reaction involving metamorphic minerals (*e.g.*, Ridley & Thompson 1986). At the same time, there are few experimental data pertaining to reaction rates that could provide support for the theoretical work of Avrami (1940, 1941), Aargaard & Helgeson (1982), Fisher (1973, 1978), Helgeson *et al.* (1970, 1984), Helgeson (1971, 1972), Lasaga (1984, 1986) and Walther & Wood (1986). To achieve progress in understanding reaction kinetics, it is essential to know much more

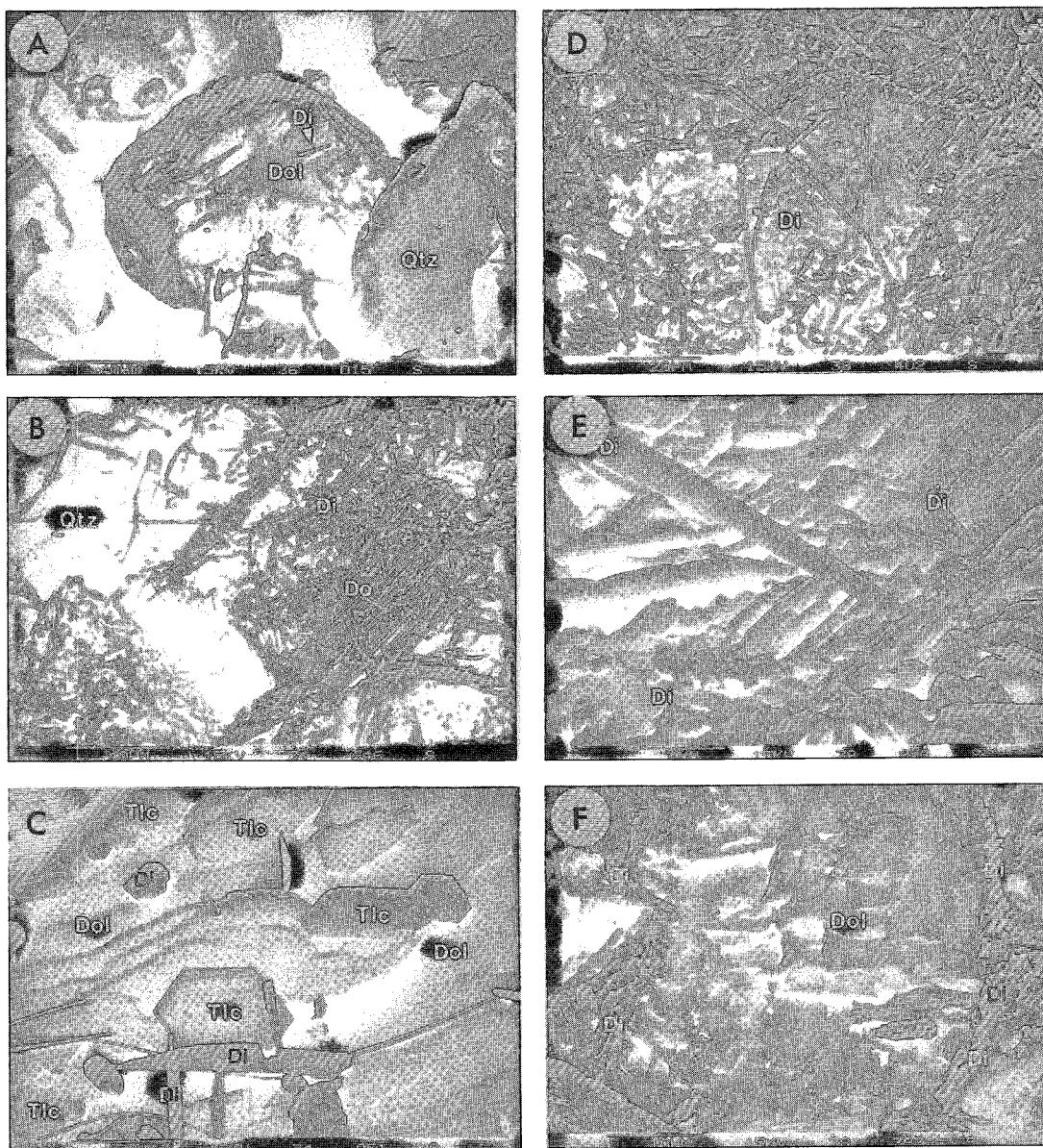


FIG. 4. Scanning electron micrograph showing the metastable formation of talc and the increase of  $\alpha$  with run duration, and the resulting armoring rim on the dolomite surfaces.  $P_{\text{tot}} = 500$  MPa,  $T = 680^\circ\text{C}$ ,  $X(\text{CO}_2)$  at start = 0.90. A. H08,  $\alpha = 1\%$ , 20 h; first crystals of Di are observable (see arrow). B. H27,  $\alpha = 27\%$ , 239 h; Dol surfaces are partly covered by Di crystals. C. H62,  $\alpha = 22\%$ , 120 h, Dol in a 5–10  $\mu\text{m}$  size fraction; metastable formation of talc (Tlc) on dolomite. D. H48,  $\alpha = 42\%$ , 1,950 h; Dol surfaces are completely covered by Di crystals. E. Armoring rim of Di crystals after 2,950 h (H50,  $\alpha = 49\%$ ). F. Same run as E; cleavage plane of a dolomite grain surrounded by a diopside rim (about 3  $\mu\text{m}$  thick).

about the rate-determining process or processes of the overall heterogeneous reactions. In general, the experimental investigation of these processes is complicated by the complexity of the mineral reactions. Therefore, we chose a simple reaction

for the experimental investigation of the kinetics despite the fact that this reaction is not very common in nature.

Experiments H08–H50 (Table 2, Fig. 5) were carried out with dolomite and quartz, both in a

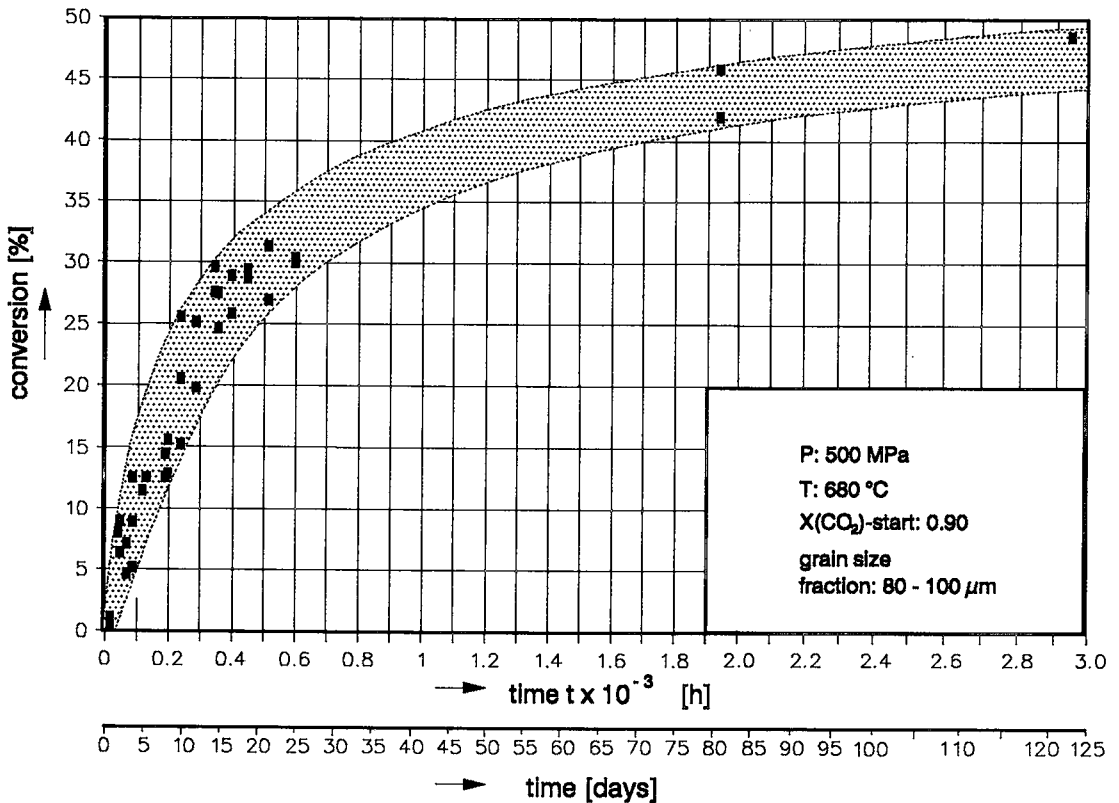


Fig. 5. Results of the unseeded runs H08 - H50. At the start of the experiment, the grain-size fraction was always 80-100 μm for both dolomite and quartz.

80-100 μm grain-size fraction. Figures 4A-F illustrate some important stages of the reaction:

- After 20 hours, the first diopside needles can be observed (Fig. 4A). During the course of the reaction, the dolomite surfaces become increasingly overgrown by diopside crystals.
- Figure 4B shows the situation after 239 hours ( $\alpha = 10\%$ ). There are still areas free of diopside on the dolomite surfaces. By this time, the metastable formation of very thin plates of talc (Tlc) can be established, as shown in Figure 4C.
- The nucleation period of diopside persists during the first 600 hours ( $\alpha = 30\%$ ), which is much longer than expected at the beginning of this investigation. The increase of conversion is almost linear during this period, as can be seen from Figure 5.
- After about 800 hours ( $\alpha = 35\%$ ), all dolomite grains are covered by diopside crystals. This diopside rim is closed, as can be seen from Figures 4D-F, after nearly 2,000 hours ( $\alpha = 45\%$ ).

On the basis of the SEM observations, we conclude that the reaction obeys a dissolution-crystallization mechanism, and we suggest also that the

reaction kinetics might be surface-controlled during the first 800 hours of the experiment. When the dolomite grains become armored, after about 800 hours, the reaction rate decreases. We must now assume, as did Tanner *et al.* (1985), that diffusion through the product layer is rate-limiting. The difference with their study is one of time. In the case of the wollastonite-producing reaction, only six hours are necessary to close the product rim under the P-T-X conditions of the experiments performed by Tanner *et al.* (1985), but more than 600 hours were necessary to close the rim in the case of the diopside-producing reaction investigated here. Between the 2,000th and 3,000th hour, the reaction rate approaches but does not reach zero. Lasaga (1986) presented a theoretical discussion of the interplay of surface-controlled processes between a reactant that becomes dissolved, and a product mineral that crystallizes from an oversaturated solution. The two-path model (Fig. 11) consists also of two interplays: 1) dolomite dissolution - diopside crystallization, and 2) quartz dissolution - diopside crystallization.

To study the influence of surfaces of the

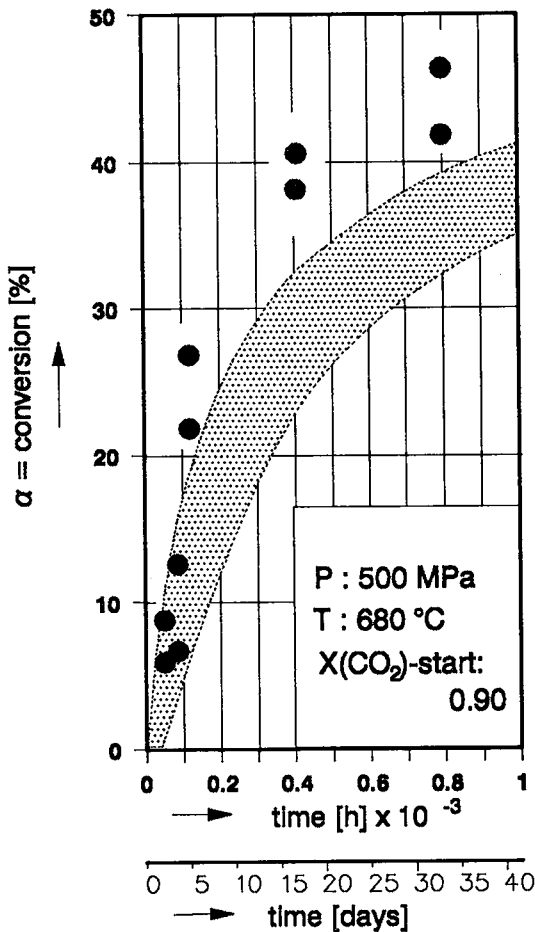


FIG. 6. Results of the unseeded runs H57 – H66, with a higher surface-area of Dol. At the beginning of the experiments, quartz was from the 80–100  $\mu\text{m}$  size fraction. The dolomite powder, however, consisted of 20 mg in 5–10  $\mu\text{m}$  size fraction and 4.22 mg in 80–100  $\mu\text{m}$  size fraction. The stippled area represents experimental results shown in Fig. 5.

reactants and product upon reaction kinetics, three types of experiments were carried out: runs with enlarged surface-area of dolomite (Table 3a), runs with added diopside crystals (Table 3b) and runs with an enlarged surface-area of quartz (Table 3c). The results of these runs (Figs. 6–8) show that a distinct increase of reaction rate is observable after 120 hours, as the surface area of dolomite increases (Fig. 6). A similar effect is seen in the case of diopside-seeded runs (Fig. 7), and no increase of reaction rate can be observed in the case of increased surface-area of quartz (Fig. 8). [The reason for the lower rate of the overall reaction (see runs H71 and H72 in Fig. 8) might be the rapid dissolution of quartz, which could have reduced

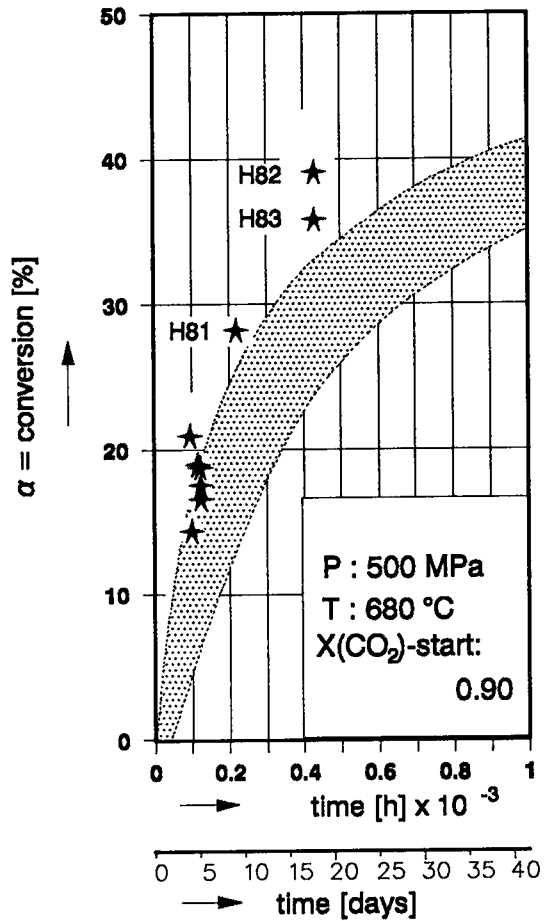


FIG. 7. Results of the diopside-seeded runs H73 – H83. At the beginning of the experiments, quartz and dolomite were always from the 80–100  $\mu\text{m}$  size fraction, with about 5 mg of diopside of a size fraction smaller than 10  $\mu\text{m}$ . The stippled area represents experimental results shown in Fig. 5.

the dissolution rate of dolomite. This can be determined, however, only when values of concentration can be measured.] Thus, at the P–T–X conditions applied in this study, it is evident that the reaction is surface-controlled. This result is in agreement with those of Tanner *et al.* (1985) and Dachs & Metz (1988). The experimental data also have shown that the interplay of path 1 (dolomite dissolution – diopside crystallization) is slower than the interplay of quartz dissolution and diopside formation (path 2). Therefore, from the experimental data and the observations made with SEM, we can point out that the processes along path 1 are rate-limiting for the overall reaction during the first 800 hours, but it is not possible to decide which

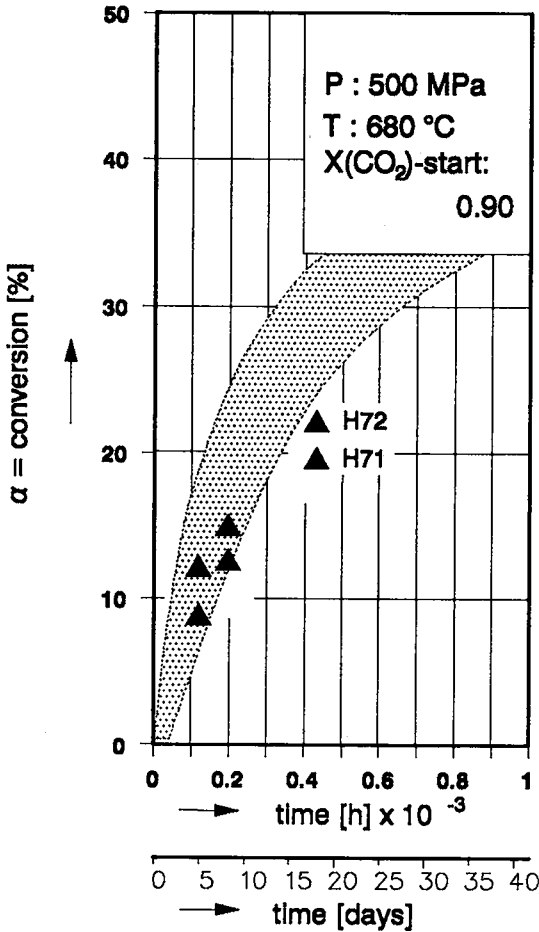


FIG. 8. Results of the unseeded runs H67 – H72, with a greater surface-area of quartz. At the beginning of experiments, 13 mg of the quartz was from a 5–10  $\mu\text{m}$  size fraction, and 2.78 mg consisted of particles 80–100  $\mu\text{m}$  across. The grains of Dol, however, were also 80–100  $\mu\text{m}$  in size. The stippled area represents experimental results shown in Fig. 5.

process involved in path 1 is rate-determining.

KINETICS: THEORETICAL

The following theoretical discussion is an attempt to understand the kinetics of path 1 in more detail. Despite the fact that there is as yet a lack of data required for many of the variables involved, we suggest that the discussion of equation A9, made in a qualitative manner and not violating the experimental results, is informative.

For the following discussion, we make the assumption, which is perhaps an oversimplification, that dolomite dissolution and diopside

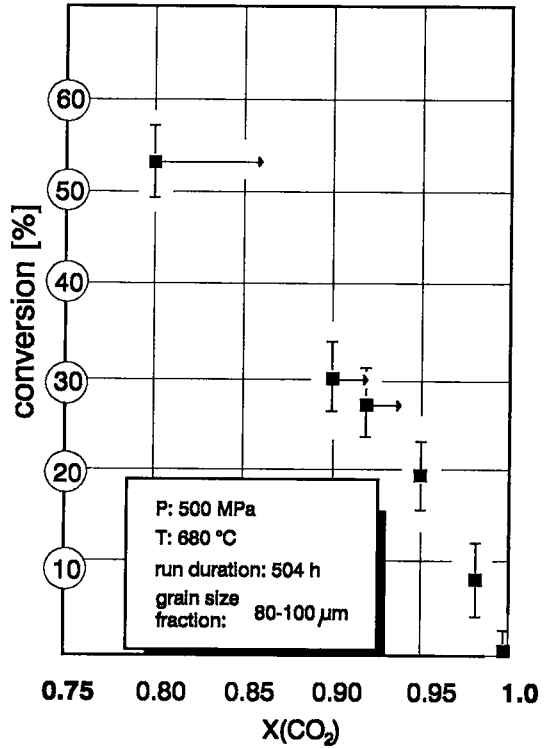


FIG. 9. Degree of conversion  $\alpha$  (unseeded runs, Tables 4 and 5) plotted as a function of the  $X(\text{CO}_2)$  values. The arrows indicate direction and magnitude of  $X(\text{CO}_2)$  shift during the run. The starting mixture of dolomite and quartz was from the 80–100  $\mu\text{m}$  size fraction in each case.

crystallization are congruent. Thus, we can write (see the appendix for a derivation):

Term 1 of equation (A9) takes into consideration

$$\frac{dc_i}{dt} = \left[ \overbrace{k_{Dol}^+ \cdot A_{Dol} \left( 1 - \frac{a_{Ca} \cdot a_{Mg}}{L_{Dol}^{*eq}} \right)}^{\text{term 1}} + \overbrace{k_{Di}^+ \cdot A_{Di} \left( 1 - \frac{a_{Ca} \cdot a_{Mg}}{L_{Di}^{*eq}} \right)}^{\text{term 2}} \right] \quad (\text{A9})$$

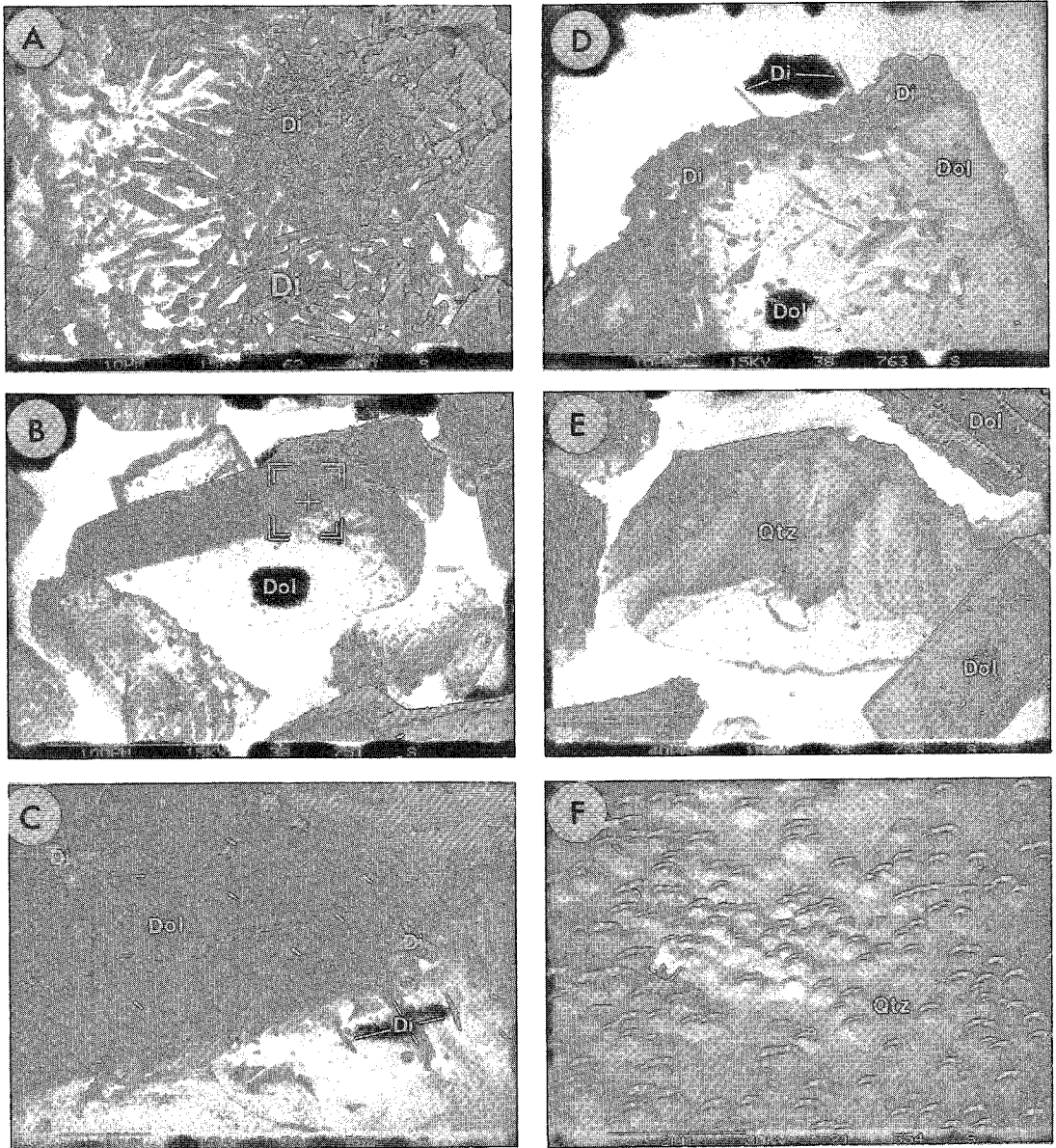


FIG. 10. A. Di crystals formed in a diopside-seeded run (H81,  $\alpha = 28\%$ ); seeds have grown, whereas new crystals of Di also have formed (see the very small ones). B. Part of a reaction mixture after 365 days run duration (run with "pure"  $\text{CO}_2$ ). Only very small crystals of Di are present. C. Marked area of B at a higher magnification; Di whiskers and etch pits (see arrows) can be seen on the Dol surface. D. On the edges of the Dol grain, crystallization of Di has increased. E. Qtz grain after 365 days run duration: sharp edges are still observable. F. Dissolution features (hillocks) on a Qtz surface after 182 days at experimental conditions.

the dissolution of dolomite, and term 2 describes the formation of diopside;  $dc_i/dt$  is the net change in concentration of species  $i$  (Ca or Mg), caused by the overall reaction, that is to say, by the interplay of dissolution and precipitation processes involved

in path 1. The parameters  $k_{\text{Dol}}^+$  and  $k_{\text{Di}}^+$  are the overall rate-constants of both processes.  $A_{\text{Dol}}$  ( $A_{\text{Di}}$ ) is the surface of dolomite (diopside).  $V$  is the volume of the fluid phase in contact with the minerals;  $a_{\text{Ca}}$ ,  $a_{\text{Mg}}$  and  $a(\text{H}^+)$  are the activities of

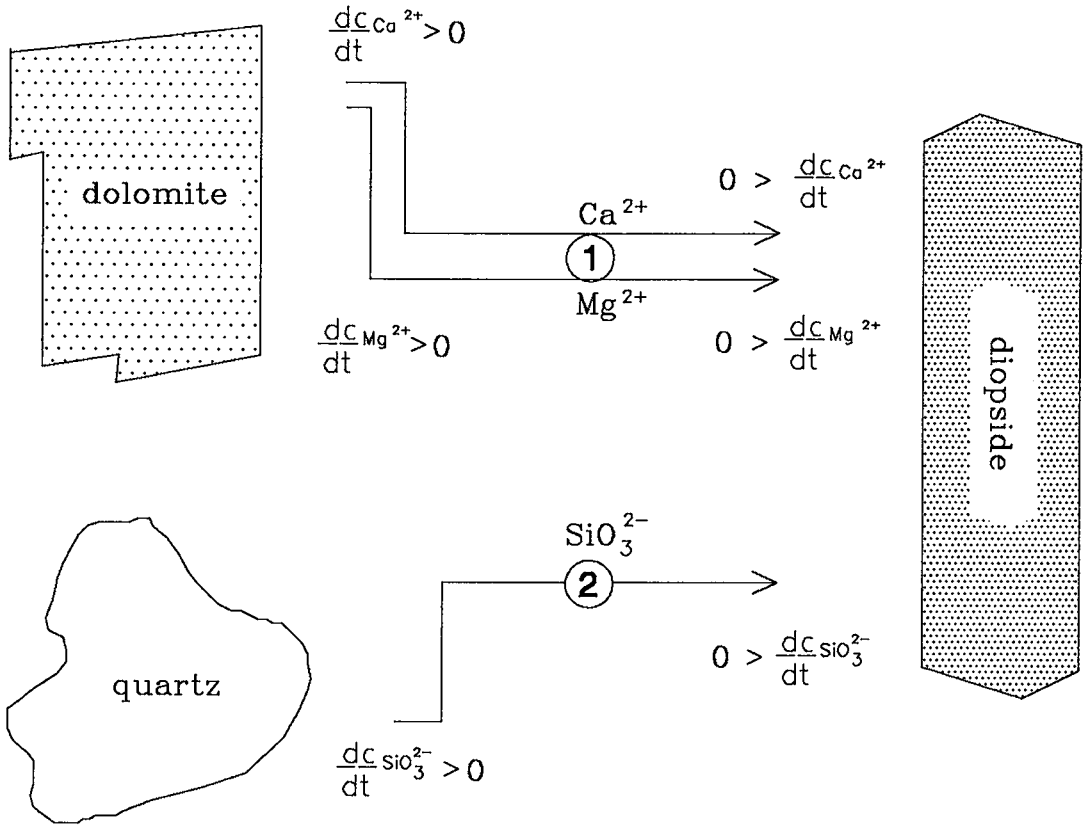


FIG. 11. Simplified schematic illustration of the "two-path model" of reaction (8). Each "path" includes the dissolution of a reactant (Dol or Qtz, respectively), the transport of dissolved species (Ca and Mg, respectively, in the case of path 1, and  $SiO_3^{2-}$  in the case of path 2), and the crystallization of diopside. The dissolution and precipitation processes are described by changes in concentration.

Ca-, Mg-species and  $H^+$  in the solution.  $L_{Di}^{*eq}$  is the reduced activity-product of diopside (dolomite) at equilibrium, which has a definite but unknown value for the P, T and  $X(CO_2)$  of the experiments carried out. We write the index \* because  $L^*$  is valid for specific constant values of  $a(CO_2)$ ,  $a(H_2O)$  and  $a_{Si}$ . The experimental results (H67-H72) have shown that an increase in the dissolution of quartz does not increase the rate of the overall reaction. This implies that  $c_{Si}$  is at a steady state after a few hours at run conditions. If this is so,  $dc_{Si}/dt$  is equal to 0, and  $c_{Si}$  is constant.

The total system of differential equations for all concentrations involved in the overall reaction has to be solved for each general case. In the case of reaction (8), however, the problem is much simpler, as mentioned above:  $c_{Si}$  has a constant value, and  $c_{Ca}$  always equals  $c_{Mg}$ , if congruent dissolution of dolomite and precipitation of diopside are assumed, respectively. Thus we can write:

$$\frac{dc_{Ca}}{dt} = \frac{dc_{Mg}}{dt} = \frac{(a(H^+))}{V} \left[ \overbrace{k_{Dol}^+ \cdot A_{Dol} \left( 1 - \frac{a_{Ca} \cdot a_{Mg}}{L_{Dol}^{*eq}} \right)}^{\text{term 1}} + \overbrace{k_{Di}^+ \cdot A_{Di} \left( 1 - \frac{a_{Ca} \cdot a_{Mg}}{L_{Di}^{*eq}} \right)}^{\text{term 2}} \right] \tag{A10}$$

The change of  $c_{\text{Ca}}(c_{\text{Mg}})$  with time is qualitatively the same as the change of the product  $c_{\text{Ca}} \cdot c_{\text{Mg}}$  (if we assume the special case in which  $c_{\text{Ca}} = c_{\text{Mg}}$ , *i.e.*, congruent behavior). Therefore, we can examine qualitatively the change of  $L^*$  with time. The outcome of this discussion is presented graphically in Figure 12.

The initial period (phase I) lasts about 20 hours, *i.e.*, from  $t_0$  to  $t_{20}$  (Fig. 12). During this time, crystallization of diopside was not detected experimentally. The concentrations of all species will increase rapidly because of the dissolution of dolomite and quartz. During  $t_0$  to  $t_{20}$ , equation (A7) and an analogous equation for quartz dissolution describe the behavior of the system.

The period of diopside nucleation begins after

about 20 hours at run conditions (see p. 7), indicated as  $t_{20}$  in Figure 12. At  $t_{20}$ , the nucleation barrier for diopside is overstepped, *i.e.*,  $L^*$  is equal or greater than  $L_{\text{Di}}^{\text{nucleation}}$ . At the time when the first crystal of diopside appears, equation (A10) describes the behavior of the system. In the following, we look upon the changes in term 1, which takes into consideration the increase of  $c_{\text{Ca}}(c_{\text{Mg}})$  resulting from the dissolution of dolomite, and term 2, which describes the decrease of  $c_{\text{Ca}}(c_{\text{Mg}})$  resulting from the formation of diopside. At the beginning of diopside formation,  $A_{\text{Dol}}$  in term 1 is much higher than  $A_{\text{Di}}$  in term 2. If at the same time  $k_{\text{Dol}}^+$  is not too different from  $k_{\text{Di}}^+$ , the first term of equation (A10) should be, therefore, determinative for  $L^*$ . As long as this is the case,

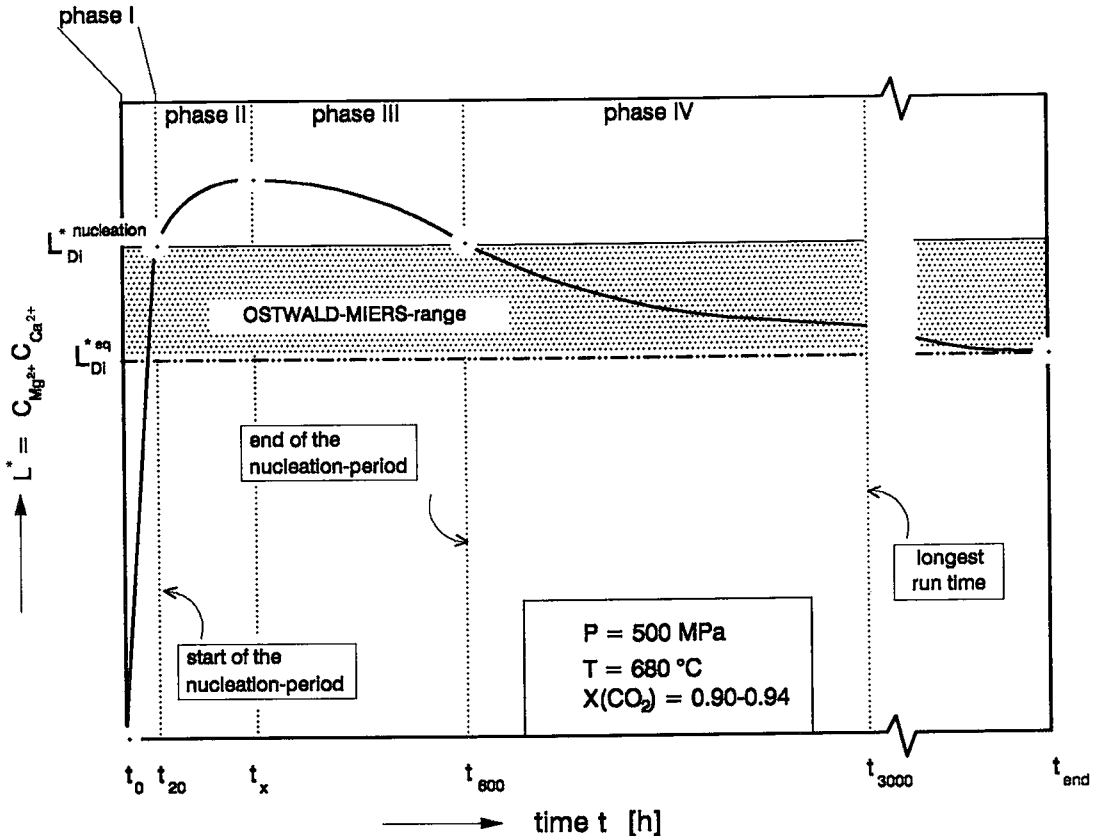


FIG. 12. Concentration product  $L^*$  plotted as a function of time  $t$ , deduced from eq. (A10). Phase I: initial period (only dissolution of quartz and dolomite); phases II, III: period of diopside nucleation; phase IV: the reaction is controlled by the dissolution of dolomite or transport processes, respectively. ( $L_{\text{Di}}^{\text{eq}}$  = value of the reduced concentration-product of diopside at equilibrium;  $L_{\text{Di}}^{\text{nucleation}}$  = value of nucleation barrier of diopside. Ostwald-Miers range = crystal growth occurs, but no nucleation is possible). For more detailed information, see text.

the increase of  $L^*$ , i.e.,  $c_{Ca}$  and  $c_{Mg}$ , in the fluid phase, which originates from the dissolution of dolomite, exceeds the decrease of  $L^*$  originating from the consumption of Ca and Mg, respectively, by the nucleation and growth of diopside. In other words,  $L^*$  increases further, but its slope is reduced continuously starting at  $t_{20}$ . From  $t_{20}$  to  $t_x$  ( $t_x$  is defined below), the kinetics of the overall reaction should be controlled by the processes of crystallization of the diopside and not by the dissolution of dolomite. This period is called phase II (Fig. 12).

This conclusion is supported by an important observation made during SEM studies: in seeded runs (H73–H83, Fig. 10A), it is commonly possible to observe not only the seeds, which have grown bigger, but also newly formed diopside crystals, which have nucleated and grown at the same time. This shows that the concentration product  $L^*$  was not only greater than  $L_{Di}^{*eq}$  but also higher than or equal to  $L_{Di}^{*nucleation}$ . This is achievable only if the dissolution of the dolomite is faster than the nucleation and growth of diopside. The length of time that this state of affairs lasts will be determined by the extent to which the assumption of similar rate-constants for  $k_{Dol}^+$  and  $k_{Di}^+$  is correct. Equation (A10) does not consider any process of nucleation explicitly. Therefore, it is necessary, for the formulation of a more detailed model, to consider also the consumption of Ca and Mg species by processes of nucleation. It will be essential for future work to account for nucleation in equation (A10).

As the reaction proceeds,  $A_{Dol}$  will progressively decrease while  $A_{Di}$  will increase, conditioned by the continued nucleation and growth of diopside. At the same time,  $a_{Ca} \cdot a_{Mg}/L_{Di}^{*eq}$  approaches 1, and  $a_{Ca} \cdot a_{Mg}/L_{Di}^{*eq}$  becomes increasingly greater than 1; this means that the absolute value of term 1 will decrease, whereas the absolute value of term 2 will increase. As a result of this process, the absolute values of term 1 and term 2 will become equal at a certain point. At the time when this occurs,  $dc_{Ca}/dt = dc_{Mg}/dt = 0$ . The time that this happens is not determinable by our experiments. Therefore, it is called  $t_x$  here (Fig. 12). At  $t_x$ , the consumption of Ca and Mg species at the diopside–fluid interfaces equals that of species production at the dolomite–fluid interfaces. It is obvious that  $dL^*/dt$  also is zero. Therefore  $L^*$  as a function of  $t$  has a maximum at  $t_x$ .

With further conversion,  $A_{Dol}$  will decrease, and the absolute value of term 1 will therefore become progressively smaller, whereas  $A_{Di}$  and the absolute value of term 2 will increase. In general the production of Ca- and Mg-bearing species by dissolution of dolomite is less than the consumption

of these species by diopside formation. The slope of the curve showing  $L^*$  as a function of time will therefore become negative at  $t$  greater than  $t_x$ . The change of slope indicates that the rate-controlling step of the overall reaction has changed. For times greater than  $t_x$ , the dissolution of dolomite is slower than the nucleation and growth of diopside. That is to say, beyond  $t_x$  it is the dissolution of dolomite and not the nucleation and growth of diopside that is the rate-limiting process of the overall reaction (8). The period between  $t_x$  and  $t_{600}$  is called phase III.

SEM studies of reaction mixtures after about 600 hours show that the nucleation process of diopside has come to an end. From  $t_{600}$  on, only the growth of diopside crystals could be observed. This observation can be understood by considering the decrease of  $A_{Dol}$  by dissolution and, in addition, the armoring effect of the diopside crystals, which cuts down the surface area of dolomite in direct contact with the fluid phase. Consequently,  $c_{Ca}$  and  $c_{Mg}$  will decrease so much that the value of  $L^*$  has to become smaller than  $L_{Di}^{*nucleation}$ . On the other hand,  $c_{Si}$  should still be constant, because all quartz surfaces are still free. During the further course of the reaction, the concentration product  $L^*$  will converge with  $L_{Di}^{*eq}$ . The period between  $t_{600}$  and  $t_{3000}$  (longest-duration experiment) is called phase IV.

The assumption made earlier, that the reaction rate is not transport-controlled, is valid so long as the rim of diopside crystals around all dolomite grains is not closed. As soon as this is the case, the diffusion of dissolved species through the armoring rim will be rate-limiting. The rate-determining process has changed again.

#### MECHANISM AND RATE UNDER ALMOST WATER-FREE CONDITIONS

An SEM examination of reaction mixtures held for nearly 1,000 hours at run conditions shows that the conversion decreases drastically under almost water-free conditions (Lüttge 1985; see also Fig. 9). However, in the case of a significant overstepping of the reaction (150 – 200°C), the reaction rate is faster (Table 5, VI/7 and VI/9). With respect to natural systems, the latter conditions may not be very relevant. In order to have readily perceptible conversion in the presence of nearly pure  $CO_2$  with an overstepping of only 60°C or 80°C, respectively, (Table 5, runs H84, H85), it was necessary to have run durations of up to one year (8,760 hours). The SEM photos (Figs. 10B–F) show some characteristic aspects of the reaction mechanism operating under “dry” conditions. The reaction mixtures from which these pictures were made represent a

run duration of 4,368 or 8,760 hours, respectively. Both dolomite and quartz clearly show dissolution features such as etch pits (Fig. 10C), hillocks (Fig. 10F), and slightly rounded edges and corners. The diopside crystals nucleate and grow at the same sites, but exclusively on dolomite surfaces (Figs. 10C, D). The habit of these diopside crystals (Fig. 10D) differs greatly from that observed in reaction mixtures formed with a fluid phase containing water. It appears that the number of diopside whiskers has increased (Fig. 10C). Our observations are consistent with a dissolution - crystallization mechanism (Lüttge *et al.* 1987). This result is not in agreement with studies of the reaction  $1 \text{ calcite} + 1 \text{ quartz} = 1 \text{ wollastonite} + 1 \text{ CO}_2$  done by Kridelbaugh (1973), who postulated a mechanism of solid-state diffusion involving calcium, silicon and oxygen, with diffusion of oxygen as the most likely rate-determining step.

From the SEM photos of the dissolution-crystallization textures, we assume that small amounts of water, which are adsorbed on the reactant surfaces (*cf.* Steinike *et al.* 1985, Moore & Rose 1973), are responsible for the dissolution. The catalytic effect of water is well known and has been discussed in detail by Rubie (1986). On the other hand,  $\text{CO}_2$  should not be able to break bonds in silicate minerals, *e.g.*, quartz, on account of the absence of a dipole, and the small quadrupole moment of  $\text{CO}_2$ . By contrast, Novgorodov (1975) inferred (by extrapolation) a solubility of  $\text{SiO}_2$  of 0.0166 wt.% in pure  $\text{CO}_2$  (300 MPa and 700°C) from studies of quartz solubility in  $\text{CO}_2$ - $\text{H}_2\text{O}$  mixtures. The dependence of conversion on the  $X(\text{CO}_2)$  value can be shown experimentally (Table 4, Fig. 9). Note that the results are perhaps somewhat influenced by the small decrease in the degree of overstepping of the temperature [10°C between  $X(\text{CO}_2) = 0.87$  and  $X(\text{CO}_2) = 0.98$ ]. However, these results are in close agreement with those of Tanner *et al.* (1985).

Solid-state diffusion will always operate at high temperatures, but in comparison with a simultaneous mechanism of transport of dissolved species through a fluid phase, solid-state diffusion is less effective, because of the higher activation energies required. At the temperatures used for these experiments, solid-state diffusion is a much slower process than diffusion through the fluid phase and, therefore, is not rate-limiting. Thus it follows that the rate-determining process is evidently a dissolution-precipitation mechanism, even under "dry" conditions and at temperatures up to at least 700°C.

Drier conditions than those used in our experiments with "pure"  $\text{CO}_2$  should not be expected to be very common in crustal rocks. If we take into

consideration the fact that the reaction consists of a dissolution-crystallization mechanism even under such  $\text{H}_2\text{O}$ -poor conditions, we can agree that most metamorphic reactions in nature are controlled by water-rock interactions, and not by solid-state diffusion. Moreover, the formation of diopside from dolomite and quartz, even under such  $\text{CO}_2$ -rich conditions, is rapid in comparison with geological time, *i.e.*, it takes place within decades or centuries, instead of millennia.

It is important to determine whether or not the results obtained from the experiments on mineral powders will hold also in natural systems, in view of critical points that have been raised (*e.g.*, Thompson & Rubie 1985). Therefore, a comparison of the results given above with those of experiments with cylinders of rocks has been carried out (Lüttge & Metz, in prep.).

#### SUMMARY

In summary, we conclude that a dissolution-crystallization mechanism is operative throughout the entire range of  $X(\text{CO}_2)$  investigated experimentally. This is the case even if there is only a very small amount of water present. During the course of the experiments on powders, the overall reaction is characterized by the change of the rate-limiting processes during the first 2,000 hours of run duration:

1. The reaction is interface-controlled during the first 1,000 hours of the experiment. This stage includes an initial period of dissolution of both reactants (~20 hours). At the beginning of the nucleation period the interplay between dissolution of dolomite and crystallization of diopside is determinative. In this stage, (from  $t_{20}$  to  $t_x$ ), the nucleation and growth of diopside determine the rate of the reaction. After  $t_x$  (maximum value of the concentration product), the rate is controlled by the dissolution of dolomite. This period lasts up to nearly 1,000 hours.
2. When all dolomite grains are armored by diopside crystals, *i.e.*, after about 1,000 hours, the rate-determining step changes again. Now the overall reaction is transport-controlled, *i.e.*, the diffusion of dissolved species through the diopside rim is rate-limiting. This process is, of course, much slower than the interface-controlled processes. After 1,000 hours, nearly 40% conversion can be observed. The next 2,000 hours give only an additional 20% of reaction progress.

#### ACKNOWLEDGEMENTS

The authors thank M. Gottschalk, W. Bayh, E. Dachs, S.M. Fortier, W. Heinrich, H.W. Alten,

J.V. Chernosky, and an anonymous reviewer for critical comments and helpful discussions, which considerably improved this paper. We also are very grateful to C. Hemleben and H. Hüttemann for providing SEM facilities, R. Schulz for his manifold assistance during the performance of this study, M. Mangliers, J. Mällich and N. Walker for technical assistance and preparatory work. We express our thanks to S.M. Fortier and L. Vantine for linguistic improvements to the text, and to Mrs. A. Metz for the excellent and fast typing and retyping of the manuscript. This work forms part of the research program "Kinetics of rock- and mineral-forming processes" of the Deutsche Forschungsgemeinschaft. Funds were provided by this institution and are gratefully acknowledged.

## REFERENCES

- AARGAARD, P. & HELGESON, H.C. (1982): Thermodynamic and kinetic constraints on reaction rates among minerals and aqueous solutions. I. Theoretical considerations. *Am. J. Sci.* **282**, 237-285.
- AVRAMI, M. (1940): Kinetics of phase change. II. Transformation - time relations for random distribution of nuclei. *J. Chem. Phys.* **8**, 212-224.
- \_\_\_\_\_ (1941): Kinetics of phase change. III. Granulation, phase change, and microstructure. *J. Chem. Phys.* **9**, 177-184.
- BERNER, R.A. (1978): Rate control of mineral dissolution under earth surface conditions. *Am. J. Sci.* **278**, 1235-1252.
- \_\_\_\_\_ & HOLDREN, G.R., Jr. (1979): Mechanism of feldspar weathering. II. Observations of feldspars from soils. *Geochim. Cosmochim. Acta* **43**, 1173-1186.
- \_\_\_\_\_ & MORSE, J.W. (1974): Dissolution kinetics of calcium carbonate in sea water. IV. Theory of calcite dissolution. *Am. J. Sci.* **274**, 108-134.
- \_\_\_\_\_ & SCHOTT, J. (1982): Mechanism of pyroxene and amphibole weathering. II. Observations of soil grains. *Am. J. Sci.* **282**, 1214-1231.
- \_\_\_\_\_, SJÖBERG, E.L., VELBEL, M.A. & KROM, M.D. (1980): Dissolution of pyroxenes and amphiboles during weathering. *Science* **207**, 1205-1206.
- BLENCOE, J.G., MERKEL, G.A. & SEIL, M.K. (1982): Thermodynamics of crystal - fluid equilibria, with applications to the system  $\text{NaAlSi}_3\text{O}_8 - \text{CaAl}_2\text{Si}_2\text{O}_8 - \text{SiO}_2 - \text{NaCl} - \text{CaCl}_2 - \text{H}_2\text{O}$ . In *Advances in Physical Geochemistry 2* (S.K. Saxena, ed.). Springer-Verlag, New York (191-222).
- BLUM, A.E., YUND, R.A. & LASAGA, A.C. (1990): The effect of dislocation density on the dissolution rate of quartz. *Geochim. Cosmochim. Acta* **54**, 283-297.
- DACHS, E. & METZ, P. (1988): The mechanism of the reaction  $1 \text{ tremolite} + 3 \text{ calcite} + 2 \text{ quartz} = 5 \text{ diopside} + 3 \text{ CO}_2 + 1 \text{ H}_2\text{O}$ : results of powder experiments. *Contrib. Mineral. Petrol.* **100**, 542-551.
- EUGSTER, H.P. (1982): Rock-fluid equilibrium systems. In *High-Pressure Researches in Geoscience*. E. Schweizerbart'sche Verlagsbuchhandlung, Stuttgart (501-518).
- \_\_\_\_\_ (1986): Minerals in hot water. *Am. Mineral.* **71**, 655-673.
- \_\_\_\_\_ & BAUMGARTNER, L. (1987): Mineral solubilities and speciation in supercritical metamorphic fluids. In *Thermodynamic Modeling of Geological Materials: Minerals, Fluids and Melts* (I.S.E. Carmichael & H.P. Eugster, eds.). *Rev. Mineral.* **17**, 367-403.
- FEIN, J.B. & WALTHER, J.V. (1987): Calcite solubility in supercritical  $\text{CO}_2\text{-H}_2\text{O}$  fluids. *Geochim. Cosmochim. Acta* **51**, 1665-1673.
- FISHER, G.W. (1973): Nonequilibrium thermodynamics as a model for diffusion-controlled metamorphic processes. *Am. J. Sci.* **273**, 897-924.
- \_\_\_\_\_ (1978): Rate laws in metamorphism. *Geochim. Cosmochim. Acta* **42**, 1035-1050.
- GOTTSCHALK, M. (1990): *Intern konsistente thermodynamische Daten im System  $\text{SiO}_2\text{-Al}_2\text{O}_3\text{-CaO-MgO-K}_2\text{O-Na}_2\text{O-H}_2\text{O-CO}_2$* . Ph.D. dissertation, Universität Tübingen, Tübingen, Germany.
- GREENWOOD, H.J. (1963): The synthesis and stability of anthophyllite. *J. Petrol.* **4**, 317-351.
- HEIMANN, R.B. (1975): *Auflösung von Kristallen*. Springer, Wien.
- HEINRICH, W., METZ, P. & BAYH, W. (1986): Experimental investigation of the mechanism of the reaction:  $1 \text{ tremolite} + 11 \text{ dolomite} = 8 \text{ forsterite} + 13 \text{ calcite} + 9 \text{ CO}_2 + 1 \text{ H}_2\text{O}$ . An SEM study. *Contrib. Mineral. Petrol.* **93**, 215-221.
- \_\_\_\_\_, \_\_\_\_\_ & GOTTSCHALK, M. (1989): Experimental investigation of the kinetics of the reaction  $1 \text{ tremolite} + 11 \text{ dolomite} = 8 \text{ forsterite} + 13 \text{ calcite} + 9 \text{ CO}_2 + 1 \text{ H}_2\text{O}$ . *Contrib. Mineral. Petrol.* **102**, 163-173.
- HELGESON, H.C. (1971): Kinetics of mass transfer among silicates and aqueous solutions. *Geochim. Cosmochim. Acta* **35**, 421-469.

- \_\_\_\_\_ (1972): Kinetics of mass transfer among silicates and aqueous solutions: correction and clarification. *Geochim. Cosmochim. Acta* **36**, 1067-1070.
- \_\_\_\_\_, BROWN, T.H., NIGRINI, A. & JONES, T.A. (1970): Calculation of mass transfer in geochemical processes involving aqueous solutions. *Geochim. Cosmochim. Acta* **34**, 569-592.
- \_\_\_\_\_, MURPHY, W.M. & AARGAARD, P. (1984): Thermodynamic and kinetic constraints on reaction rates among minerals and aqueous solutions. II. Rate constants, effective surface area and the hydrolysis of feldspar. *Geochim. Cosmochim. Acta* **48**, 2405-2432.
- KÄSE, H.-R. & METZ, P. (1980): Experimental investigation of the metamorphism of siliceous dolomites. IV. Equilibrium data for the reaction: 1 Diopside + 3 Dolomite  $\rightleftharpoons$  2 Forsterite + 4 Calcite + 2 CO<sub>2</sub>. *Contrib. Mineral. Petrol.* **73**, 151-159.
- KRIDELBAUGH, S.J. (1973): The kinetics of the reaction: calcite + quartz = wollastonite + carbon dioxide at elevated temperatures and pressures. *Am. J. Sci.* **273**, 757-777.
- LASAGA, A.C. (1984): Chemical kinetics of water - rock interactions. *J. Geophys. Res.* **89**, 4009-4025.
- \_\_\_\_\_ (1986): Metamorphic reaction rate laws and development of isograds. *Mineral. Mag.* **50**, 359-373.
- LÜTTGE, A. (1985): *Experimentelle Untersuchungen zum Mechanismus der Reaktion: 1 Dolomit + 2 Quartz = 1 Diopsid + 2 CO<sub>2</sub>*. Diplomarbeit, Inst. f. Mineralogie, Petrologie u. Geochemie, Univ. Tübingen, Tübingen, Germany.
- \_\_\_\_\_, METZ, P. & REHLÄNDER, R. (1987): Concepts of the mechanism of decarbonation reactions in siliceous carbonates. *Terra Cognita* **7**, 253 (abstr.).
- MATTHEWS, A. (1980): Influences of kinetics and mechanism in metamorphism: a study of albite crystallisation. *Geochim. Cosmochim. Acta* **44**, 387-402.
- \_\_\_\_\_ (1985): Kinetics and mechanisms of the reaction of zoisite to anorthite under hydrothermal conditions: reaction phenomenology away from the equilibrium region. *Contrib. Mineral. Petrol.* **89**, 110-121.
- MOORE, G.S.M. & ROSE, H.E. (1973): The structure of powdered quartz. *Nature* **242**, 187-190.
- NOVGORODOV, P.G. (1975): Solubility of quartz in H<sub>2</sub>O-CO<sub>2</sub> mixtures at 700°C and pressures of 3 and 4 kbar. *Geochem. Intern.* **12**(5), 122-126.
- PETROVICH, R. (1981a): Kinetics of dissolution of mechanically comminuted rock-forming oxides and silicates. I. Deformation and dissolution of quartz under laboratory conditions. *Geochim. Cosmochim. Acta* **45**, 1665-1674.
- \_\_\_\_\_ (1981b): Kinetics of dissolution of mechanically comminuted rock-forming oxides and silicates. II. Deformation and dissolution of oxides and silicates in the laboratory and at the Earth's surface. *Geochim. Cosmochim. Acta* **45**, 1675-1686.
- PETROVIĆ, R., BERNIER, R.A. & GOLDBABER, M.B. (1976): Rate control in dissolution of alkali feldspars. I. Study of residual feldspar grains by X-ray photoelectron spectroscopy. *Geochim. Cosmochim. Acta* **40**, 537-548.
- RIDLEY, J. & THOMPSON, A.B. (1986): The role of mineral kinetics in the development of metamorphic microtextures. In *Fluid - Rock Interactions during Metamorphism* (J.V. Walther & B.J. Wood, eds.). Springer-Verlag, New York (154-193).
- RIMSTIDT, J.D. & BARNES, H.L. (1980): The kinetics of silica - water reactions. *Geochim. Cosmochim. Acta* **44**, 1683-1699.
- RUBIE, D.C. (1986): The catalysis of mineral reactions by water and restrictions on the presence of aqueous fluid during metamorphism. *Mineral. Mag.* **50**, 399-415.
- \_\_\_\_\_ & BREARLEY, A.J. (1987): Metastable melting during the breakdown of muscovite + quartz at 1 kbar. *Bull. Minéral.* **110**, 533-549.
- SCHRAMKE, J.A., KERRICK, D.M. & LASAGA, A.C. (1987): The reaction muscovite + quartz = andalusite + K-feldspar + water. I. Growth kinetics and mechanism. *Am. J. Sci.* **287**, 517-559.
- STEINIKÉ, U., HENNIG, H.P. & EBERT, I. (1985): Beziehungen zwischen Strukturveränderungen und Sorption am mechanisch aktivierten Quarz. *Z. phys. Chem.* **266**(2), 302-310.
- TANNER, S.B., KERRICK, D.M. & LASAGA, A.C. (1985): Experimental kinetic study of the reaction: calcite + quartz  $\rightleftharpoons$  wollastonite + carbon dioxide, from 1 to 3 kilobars and 500 to 850°C. *Am. J. Sci.* **285**, 577-620.
- THOMPSON, A.B. & RUBIE, D.C., eds. (1985): *Metamorphic Reactions*. Advances in Physical Geochemistry, Vol. 4. Springer-Verlag, New York.
- TOYOCOM (1975): Quality standards for the inclusions of TOYO quartz. *TOYOCOM Equipment Co. Ltd., Tokyo, Tech. Bull. C-5*.

VAN LIER, J.A., DE BRUYN, P.L. & OVERBEEK, J.T.G. (1960): The solubility of quartz. *J. Phys. Chem.* **64**, 1675-1682.

WALTHER, J.V. & ORVILLE, P.M. (1982): Volatile production and transport in regional metamorphism. *Contrib. Mineral. Petrol.* **79**, 252-257.

\_\_\_\_\_ & \_\_\_\_\_ (1983): The extraction-quench technique for determination of the thermodynamic properties of solute complexes: application to quartz solubility in fluid mixtures. *Am. Mineral.* **68**, 731-741.

\_\_\_\_\_ & WOOD, B.J., eds. (1986): *Fluid - Rock Interactions during Metamorphism*. Advances in Physical Geochemistry, Vol. 5. Springer-Verlag, New York.

WINKLER, H.G.F. (1979): *Petrogenesis of Metamorphic Rocks* (5th ed.). Springer-Verlag, New York.

WOODLAND, A.B. & WALTHER, J.V. (1987): Experimental determination of the solubility of the assemblage paragonite, albite, and quartz in supercritical H<sub>2</sub>O. *Geochim. Cosmochim. Acta* **51**, 365-372.

Received December 17, 1990, revised manuscript accepted May 30, 1991.

## APPENDIX

In cases far removed from equilibrium, it is possible to write the following equation for the dissolution of a mineral  $\Theta$  (Lasaga 1984):

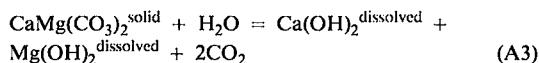
$$\frac{dc_i}{dt} = \frac{A_\Theta}{V} \cdot \nu_{i\Theta} \cdot k_\Theta^+ (a(H^+))^{n_\Theta} \quad (A1)$$

where  $dc_i/dt$  is the change in concentration of species  $i$  in the fluid phase with respect to the change in time,  $k_\Theta^+$  is the overall rate-constant of the dissolution process of mineral  $\Theta$ , and  $A_\Theta$  is its surface.  $V$  is the volume of the solution (fluid phase) in contact with mineral  $\Theta$ . Equation (A1) should hold for the dissolution of quartz and dolomite, respectively, at the very beginning of the experiments. As equilibrium is approached between a reactant and the solution, the rate of precipitation will become more and more important. Lasaga (1984) proposed equation (A2), which takes precipitation into account, in addition to dissolution:

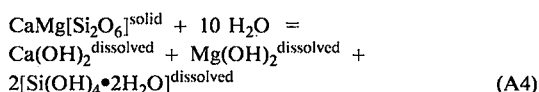
$$\frac{dc_i}{dt} = \frac{A_\Theta}{V} \cdot \nu_{i\Theta} \cdot k_\Theta^+ \cdot (a(H^+))^{n_\Theta} - \frac{A_\Theta}{V} \cdot \nu_{i\Theta} \cdot k_\Theta^{\frac{Q_m}{K_{eq}}} (a(H^+))^{n_\Theta} \quad (A2)$$

where  $dc_i/dt$  is now the net change in concentration of species  $i$  in the solution that is in contact with a mineral  $\Theta$ .  $Q$  is the activity quotient, and  $K_{eq}$  is the value of this quotient in the case of equilibrium. Both  $m$  and  $n$  are constants that usually have to be determined experimentally. Following Lasaga (1984), it is assumed here that  $m$  and  $n_\Theta$  equal 1 as a first approximation. The stoichiometric coefficient  $\nu$  equals 1 also if congruent dissolution and precipitation are assumed. Equation (A2) also should hold for crystal growth of the mineral  $\Theta$  from an oversaturated solution, e.g., for the crystallization of diopside in the case of reaction (8).

The dissolution of dolomite may be described schematically as follows:



At present, it is not possible to write a more descriptive equation, because the species in CO<sub>2</sub>-rich fluid phase are not well known (Eugster & Baumgartner 1987). We therefore use the following schematic reaction for the crystallization of diopside also:



Using equations (A2) and (A3) and inserting the activities of the dissolved species, we obtain for dolomite:

$$\frac{dc_i}{dt} = k_{Dol}^+ \frac{A_{Dol}}{V} (a(H^+)) - k_{Dol}^+ \frac{A_{Dol}}{V} (a(H^+)) \left( \frac{a_{Ca} \cdot a_{Mg} \cdot (a(\text{CO}_2))^2}{a_{Dol} \cdot (a(\text{H}_2\text{O}))^2} \right) - k_{Dol}^+ \frac{A_{Dol}}{V} (a(H^+)) \left( \frac{a_{Ca}^{eq} \cdot a_{Mg}^{eq} \cdot (a(\text{CO}_2))^{2 \cdot eq}}{a_{Dol}^{eq} \cdot (a(\text{H}_2\text{O}))^{2 \cdot eq}} \right) \quad (A5)$$

If  $X(\text{CO}_2)$  and  $X(\text{H}_2\text{O})$  are nearly constant, as can be approximated in the case of the experiments performed here,  $a(\text{CO}_2)$  and  $a(\text{H}_2\text{O})$  can be assumed to be constant also. In addition, we consider also, as a first approximation, that  $a_{Si}$  has a constant value over time (steady state), and that  $a_{Ca}$  is equal to  $c_{Ca}$  ( $a_{Mg}$  is equal to  $c_{Mg}$ ). This simplification is allowed if we use the Henrian standard state (e.g., Blencoe *et al.* 1982), which is justified if the concentrations of dissolved species in the fluid phase are not too high. In our case, it is reasonable to assume Henrian behavior. Even if there is a deviation from Henrian behavior, the statements made from equation A9 (A10) are still qualitatively correct. The activities of dolomite,  $a_{Dol}$ , and diopside,  $a_{Di}$ , equal 1 as long as both minerals remain pure phases. For this case, equation (A5) will become much simpler:

$$\frac{dc_i}{dt} = k_{Dol}^+ \frac{A_{Dol}}{V} (a(H^+)) - k_{Dol}^+ \frac{A_{Dol}}{V} (a(H^+)) \left( \frac{a_{Ca} \cdot a_{Mg}}{a_{Ca}^{eq} \cdot a_{Mg}^{eq}} \right) \quad (A6)$$

The product  $a_{Ca}^{eq} \cdot a_{Mg}^{eq}$  is the reduced activity-product in equilibrium of Ca- and Mg-bearing species in the solution, which we call  $L_{Di}^{*eq}$ . We write the index \* because  $L^*$  is valid for specific constant values of  $a(\text{CO}_2)$ ,  $a(\text{H}_2\text{O})$  and  $a_{Si}$ . However, note that  $L_{Dol}^{*eq}$  is clearly a function of P, T,  $X(\text{CO}_2)$  and  $a_{Si}$ . Under the experimental conditions applied,  $L_{Dol}^{*eq}$  has a definite but unknown value. Equation (A6) can be rewritten:

$$\frac{dc_i}{dt} = k_{Dol}^+ \frac{A_{Dol}}{V} (a(H^+)) \left( 1 - \frac{a_{Ca} \cdot a_{Mg}}{L_{Dol}^{*eq}} \right) \quad (\text{A7})$$

An equation such as (A7) can also be written for the dissolution of quartz. [For a more detailed description of the dissolution of quartz, the reader should consult Van Lier *et al.* (1969), Rimstidt & Barnes (1980), Walther & Orville (1983) and Woodland & Walther (1987).] If it can be assumed that  $c_{Si}$  is at a steady state after a short period of some hours, then  $dc(\text{SiO}_2)/dt$  is equal to 0, and  $a(\text{SiO}_2)$  is constant. Using equations (A2) and (A4) in consideration of the assumption above, we can write equation (A8) for the crystallization of diopside in a manner analogous to equation (A7)

$$\frac{dc_i}{dt} = k_{Di}^+ \frac{A_{Di}}{V} (a(H^+)) \left( 1 - \frac{a_{Ca} \cdot a_{Mg}}{L_{Di}^{*eq}} \right) \quad (\text{A8})$$

Notice that  $L_{Di}^{*eq}$  is the reduced activity-product of diopside at equilibrium; it has a definite but unknown value for P, T and  $X(\text{CO}_2)$  of the experiments carried out, and the above-mentioned constant activities of  $\text{SiO}_2$  and  $\text{H}_2\text{O}$ . Now we combine equations (A7) and (A8):

$$\frac{dc_i}{dt} = \frac{(a(H^+))}{V} \left[ \overbrace{k_{Dol}^+ \cdot A_{Dol} \left( 1 - \frac{a_{Ca} \cdot a_{Mg}}{L_{Dol}^{*eq}} \right)}^{\text{term 1}} + \overbrace{k_{Di}^+ \cdot A_{Di} \left( 1 - \frac{a_{Ca} \cdot a_{Mg}}{L_{Di}^{*eq}} \right)}^{\text{term 2}} \right] \quad (\text{A9})$$

where  $dc_i/dt$  is now the net change in concentration of species  $i$  (Ca or Mg) caused by the overall reaction, that is to say, by the interplay of the dissolution of dolomite and the precipitation of diopside (path 1).